Atomic-resolution study of Mn tetramer clusters using scanning tunneling microscopy

Rong Yang, Haiqiang Yang, and Arthur R. Smith[a)]
Nanoscale and Quantum Phenomena Institute, Department of Physics and Astronomy, Ohio University, Athens, Ohio 45701

(Received 28 November 2005; accepted 8 March 2006; published online 24 April 2006)

A manganese nitride surface containing a well-ordered array of MnN-bonded manganese clusters is investigated. The clusters are composed of a quadrant array of Mn atoms forming a tetramer. Scanning tunneling microscopy is used to image and resolve the clusters into their constituent atoms and their structure and arrangement is presented. The Mn–Mn and Mn–N bond lengths are estimated from the experimental data and compared with theoretical predictions by Rao and Jena [Phys. Rev. Lett. **89**, 185504 (2002)] for free, N-doped Mn clusters. The possible effect of the bond lengths on the magnetic properties of the clusters is discussed. © *2006 American Institute of Physics*. [DOI: 10.1063/1.2197316]

As device dimensions continue to shrink, it becomes increasingly important to study magnetism at reduced size and dimensionality. This new field of nanomagnetism has prompted much research recently in a variety of material systems and by means of various experimental and theoretical methods.[1–3] Of particular interest are magnetic nanoparticles, magnetic molecules, magnetic nanowires, and magnetic nanostructures in general.[4,5]

Magnetic nanoclusters have recently been explored theoretically for their potential application to the field of dilute magnetic semiconductors. Particularly, Rao and Jena studied the magnetic properties of Mn nanoclusters in relation to their possible effects in transition-metal (Mn)-doped gallium nitride, finding that N-doped Mn clusters containing from one to five Mn atoms exhibited giant magnetic moments as large as $22\mu_B$.[6] Other theoretical work has also suggested that Mn clusters are responsible for ferromagnetism in Mn-doped GaN.[7]

Experimentally, Dhar *et al.* reported the observation of Mn clusters using cross-sectional transmission electron microscope (TEM) in Mn-doped GaN, suggesting their formation to occur for Mn concentrations at or above 10%.[8,9] It is therefore highly desirable to experimentally investigate Mn nanoclusters using methods capable of atomic-scale resolution. Such investigations can put to test recent theories of Mn-doped GaN and also provide insight into the properties of Mn nanoclusters for other possible applications.

The case of Mn is particularly interesting since, although bulk Mn metal is antiferromagnetic, bulk N-doped Mn (i.e., Mn_4N) can be *ferrimagnetic*.[10] And, when further reducing down to cluster dimensions, N-doped Mn nanoclusters can even be *ferromagnetic*.[6] In this letter, we present a unique surface of manganese nitride, on which are stabilized periodic, self-organized array of MnN-bonded Mn tetramer clusters. We explore their structural properties and discuss them in comparison with recent theoretical predictions of N-doped Mn clusters.

Previous work has reported the successful molecular beam epitaxy (MBE) growth of different phases and orientations of manganese nitride, which can be controlled by the Mn:N flux ratio and substrate temperature.[11,12] For the work described here, we produce the (001) face of Mn_3N_2 through growth on MgO(001) substrates at $T_{substrate}=450\ ^\circ C$. A Mn effusion cell and a rf-plasma N source are used to provide the elemental fluxes; details of growth of this phase and orientation can be found elsewhere.[11]

The 3:2 (Mn:N) phase and (001) orientation are verified using reflection high energy electron diffraction (RHEED) and x-ray diffraction (XRD). Briefly, the resultant bulk film structure is of the face-centered tetragonal rocksalt-type structure with *c* axis normal to the sample surface. According to the Jacobs and Kreiner model of Mn_3N_2, the *c*-plane stacking consists of a repeating sequence of two layers of MnN followed by one layer of Mn.[13] Recent neutron diffraction measurements by Leineweber *et al.* clarify Jacobs and Kreiner's earlier report, showing that Mn magnetic moments in the range of $3.38–3.75\mu_B$ are aligned ferromagnetically in the *c* planes and that they alternate antiferromagnetically from layer to layer along the *c* axis.[14] The difference in magnetic moment between Mn atoms in Mn planes (Mn1) and Mn atoms in MnN planes (Mn2) is also discussed by Leineweber *et al.* but is very small (only $\sim 0.3\mu_B$). The Néel temperature of Mn_3N_2 was reported to be ~925 K.[15]

Following MBE growth, the sample is transferred directly to the *in situ* room-temperature scanning tunneling microscope (STM). In Fig. 1(a) is presented an image of size $800\times 800\ Å^2$, showing terraces separated by monolayer-height steps. Close inspection reveals 2 types of terrace: a smooth-type terrace and a more defected-type terrace. Comparing with the ideal stacking sequence, side-view model shown in Fig. 1(c), a correlation is found between the layers having (not having) N (from the model) and the smooth-type (defected-type) terraces (in the image). Therefore, we find that the defected-type terrace (A layer) is the Mn atom layer, and the smooth-type terraces (B layers) are the MnN layers.

Calibrated step-height analysis is presented in Fig. 1(b), where the line profiles correspond to the lines shown in Fig. 1(a). This analysis allows the determination of the step heights between layers A and B1 ($h1$), layers B1 and B2 ($h2$), and layers B2 and A ($h3$), in descending order. The values are measured to be: $h1=1.33\pm 0.01$ Å; $h2$

a)Author to whom correspondence should be addressed; electronic mail: smitha2@ohio.edu

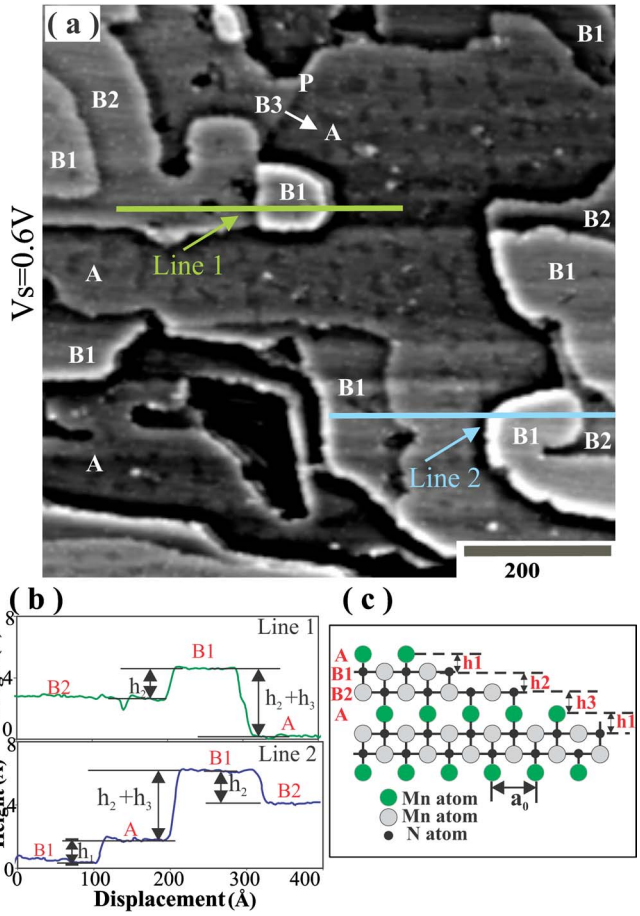

FIG. 1. (Color online) STM images of $Mn_3N_2(001)$, single line profiles, and a surface side-view model are shown. (a) A STM image of 800×800 Å^2 (V_s=0.6 V and I_t=0.8 nA). The surface stacking sequence Mn–MnN–MnN is labeled as A, B1, and B2. (b) Height profiles of line 1 and line 2. The step heights $h1=|A\rightarrow B1|=1.33\pm0.01$ Å, $h2=|B1\rightarrow B2|=2.15\pm0.01$ Å, and $h3=|B2\rightarrow A|=2.41\pm0.01$ Å. (c) Surface side-view model of $Mn_3N_2(001)$. a_0=4.21 Å. A local area background subtraction was applied to the image.

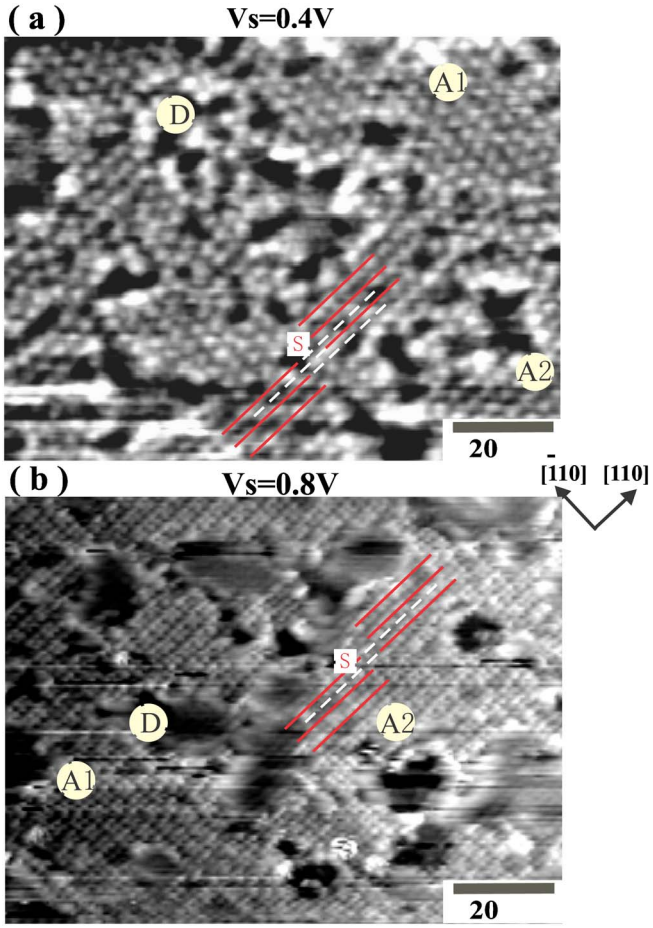

FIG. 2. (Color online) STM images of the Mn cluster layer on $Mn_3N_2(001)$ surface. (a) V_s=0.4 V and I_t=1.0 nA, gray scale range is 0.5 Å. (b) V_s=0.8 V and I_t=0.8 nA, gray scale range is 1.28 Å.

=2.15±0.01 Å; $h3$=2.41±0.01 Å. The sum=5.90±0.03 Å can be compared to the expected bulk half-lattice constant of $c/2$=6.07 Å,[11] and the difference can be attributed to a slight inward surface relaxation of ~−2.8%.

Previously, we found that for smaller Mn flux, the θ-MnN (1:1) phase, which has very similar structure to the Mn_3N_2 (3:2) phase, grows epitaxially;[11] in that case, there are only MnN layers. For larger Mn flux as presented here, there can be excess Mn at the surface forming a Mn atom layer. It is interesting that the Mn atom (A) layer appears to accumulate in the correct places to form the η-phase stacking sequence. However, an exception is seen at point P, where there is a clear boundary within a single terrace with an apparent height difference of ~0.64 Å. The B3/A boundary can be understood as a MnN growth front line within an A layer. Most likely, the concentration of A- and B-type areas depends on the arrival rates of Mn and N atoms at the surface.

The reason why the MnN terraces (B layers) appear smooth has to do with their simple 1×1 structure (as shown below). The more defective structure of the A layer is seen at higher resolution in the STM image of Fig. 2(a) where an array of tiny subnanometer-sized dots is seen, each measuring about 3 Å in diameter. There are also some defects (marked by region D), leading to some disorder; but in areas away from the defects, the tiny dots form a well-ordered, quasihexagonal array.

Based on the stacking order determined in Fig. 1, the tiny dots of the A layer should consist of Mn atoms. Their detailed structure is clarified by higher resolution STM images, as seen in Fig. 2(b), in which they are resolved as square tetramers of Mn atoms. Note: Mn states dominate over N states near the Fermi level, as established by Lambrecht *et al.*[16] The tetramers are lined up along, and with sides parallel to, ⟨110⟩. Looking perpendicular to the tetramer rows, the cluster position alternates back and forth by one tetramer spacing from row to row; this leads to the observed quasihexagonal symmetry [Fig. 2(a)]. Consequently, two types of tetramer cluster domains are observed, labeled $A1$ and $A2$.

The Mn tetramer clusters are spaced by $2a$=5.96 Å (note, $a=a_1/\sqrt{2}$, where a_1=4.21 Å is the conventional Mn_3N_2 c-plane lattice constant). Because of the two times spacing, there can also be a one tetramer shift (see points marked S in the images of Fig. 2). The apparent defects on the surface form in part due to the combined effects of domain and shift boundaries.

To better understand the Mn tetramer cluster structure, both the MnN (B-type) layer and the Mn (A-type) layer are shown in zoom-in STM images of Fig. 3. The MnN layer [Fig. 3(a)] has a simple 1×1 periodicity with Mn atoms spaced by 2.98 Å and aligned in rows along ⟨110⟩ and ⟨$\bar{1}$10⟩ directions, and it matches very well the model of Fig. 3(b).

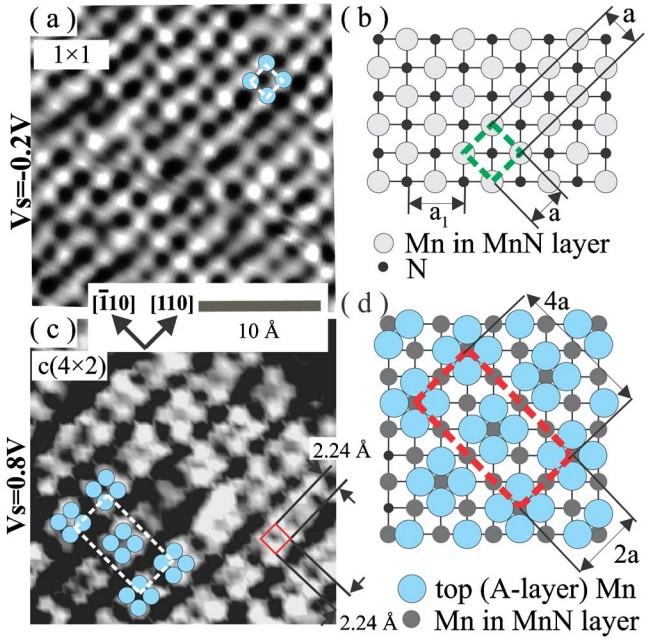

FIG. 3. (Color online) Zoom-in STM images of the MnN layer and Mn tetramer layer with corresponding surface models. (a) MnN layer, V_s=−0.2 V and I_t=1.0 nA, gray scale=0.5 Å; (b) MnN layer model; (c) Mn tetramer layer, V_s=0.8 V and I_t=0.8 nA, gray scale=1.1 Å; (d) Mn tetramer layer model.

For the STM image of the A-type (Mn) layer [Fig. 3(c)], the Mn tetramer clusters are arranged in a lattice having a $c(4\times2)$ unit cell, in excellent agreement with the model shown in Fig. 3(d). Four atoms are clearly resolved within a single tetramer.

The Mn tetramer model is shown in various side and perspective views in Fig. 4. With respect to the unstable, bulk-terminated Mn monolayer [Fig. 4(a)], the Mn layer atoms undergo reconstruction [Figs. 4(b)–4(d)]. This is qualitatively consistent with the calculations of Rao and Jena,[6] in which the formation of N-doped Mn clusters is energetically favorable. In the model of Figs. 4(b)–4(d), the four Mn atoms are displaced towards each other, forming four *intratetramer* Mn–Mn bonds, while they maintain the 4 *extratetramer* Mn–N bonds with second layer N atoms.

Direct measurement of the Mn–Mn spacing along the tetramer side gives an estimate of the Mn–Mn intratetramer bond length=2.24±0.11 Å, while the Mn–N bond length is estimated at ~1.44±0.02 Å, based on the measured step height (A→B1, Fig. 1) of 1.33 Å. It is interesting to compare these numbers with theoretical predictions of Mn–Mn

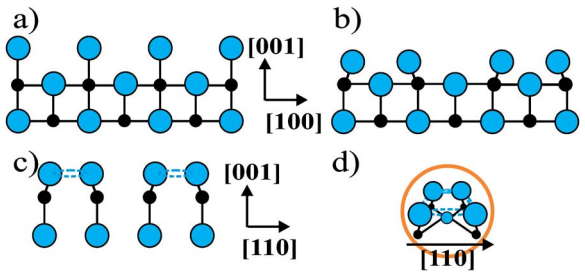

FIG. 4. (Color online) Side-view schematic models of the Mn tetramer cluster model: (a) bulklike terminated Mn layer along [100]; (b) side-view model of Mn tetramer cluster along [100]; (c) side-view model of Mn tetramer cluster along [110]; (d) perspective view of Mn tetramer cluster.

and Mn–N bond lengths for N-doped Mn clusters from the paper of Rao and Jena.[6] For clusters consisting of one N atom and from one to five Mn atoms, they found Mn–Mn distances of about 2.8±0.1 Å (6% smaller than in bulk Mn_3N_2, 2.98 Å) and Mn–N distances from 1.62 to 1.96 Å (7%–30% smaller than in bulk Mn_3N_2, 2.10 Å). Our experimentally deduced bond lengths are much smaller than bulk Mn_3N_2 values, and about 20% and from 11%–27% smaller than the theoretical free cluster predictions for Mn–Mn and Mn–N bond lengths, respectively.

Rao and Jena reported enhanced magnetic moments per Mn atom ($4.12-4.54\mu_B$) in N-doped Mn clusters.[6] Our STM findings suggest that bond lengths in N-doped Mn clusters are smaller than predicted; if so, this could potentially affect the magnetic exchange parameters and thus the magnetism of such small clusters quantitatively or even qualitatively. For example, our deduced tetramer Mn–Mn spacing (2.24±0.11 Å) is very close to the lower end of the range for Mn–Mn spacings in bulk, antiferromagnetic Mn (2.25–2.95 Å).[6] The question then becomes whether the effect of N bonding (doping) is sufficient to maintain a ferromagnetic ordering.

In conclusion, we have presented a model system consisting of Mn tetramers bonded to a MnN monolayer (substrate), and we have measured their structural properties with atomic-scale resolution. Surprisingly, the Mn–Mn and Mn–N bond lengths deduced from the STM measurements are even smaller than those of free N-doped Mn clusters predicted by Rao and Jena. Future experimental and theoretical work would be desirable to explore the magnetic properties of these MnN-bonded Mn tetramers as well as for Mn tetramers or other transition-metal atom clusters bonded to other *nonmagnetic* nitride substrates. The results could have important implications for nitride-based dilute magnetic semiconductors.

The authors acknowledge support from the National Science Foundation (Grant Nos. 9983816 and 0304314).

[1] R. P. Cowburn and M. E. Welland, Science **287**, 1466 (2000).
[2] E. Y. Vedmedenko, N. Mikuszeit, H. P. Oepen, and R. Wiesendanger, Phys. Rev. Lett. **95**, 207202 (2005).
[3] L. Y. Gorelik, R. I. Shekhter, V. M. Vinokur, D. E. Feldman, V. I. Kozub, and M. Jonson, Phys. Rev. Lett. **91**, 088301 (2003).
[4] A. N. Andriotis and M. Menon, Phys. Rev. Lett. **93**, 026402 (2004).
[5] W. Wernsdorfer and R. Sessoli, Science **284**, 133 (1999).
[6] B. K. Rao and P. Jena, Phys. Rev. Lett. **89**, 185504 (2002).
[7] M. Schilfgaarde and O. N. Mryasov, Phys. Rev. B **63**, 233205 (2003).
[8] S. Dhar, O. Brandt, A. Trampert, L. Däweritz, K. J. Friedland, K. H. Ploog, J. Keller, B. Beschoten, and G. Güntherodt, Appl. Phys. Lett. **82**, 2077 (2003).
[9] K. H. Ploog, S. Dhar, and A. Trampert, J. Vac. Sci. Technol. B **21**, 1756 (2003).
[10] W. J. Takei, R. R. Heikes, and G. Shirane, Phys. Rev. **125**, 1893 (1962).
[11] H. Q. Yang, H. Al-Brithen, A. R. Smith, E. Trifan, and D. C. Ingram, J. Appl. Phys. **91**, 1053 (2002).
[12] H. Q. Yang, H. Al-Brithen, A. R. Smith, J. A. Borchers, R. L. Cappelletti, and M. D. Vaudin, Appl. Phys. Lett. **78**, 3860 (2001).
[13] H. Jacobs and C. Stuve, J. Less-Common Met. **96**, 323 (1984).
[14] A. Leineweber, R. Niewa, H. Jacobs, and W. Kockelmann, J. Mater. Chem. **10**, 2827 (2000).
[15] M. Tabuchi, M. Takahashi, and F. Kanamaru, J. Alloys Compd. **210**, 143 (1994).
[16] W. R. L. Lambrecht, M. Prikhodko, and M. S. Miao, Phys. Rev. B **68**, 174411 (2003).